Complementarity and Young's interference fringes from two atoms

W. M. Itano, J. C. Bergquist, J. J. Bollinger, and D. J. Wineland

Time and Frequency Division, National Institute of Standards and Technology, Boulder, Colorado 80303

U. Eichmann

Max-Born-Institut for Non-linear Optics and Short Pulse Spectroscopy, Rudower Chaussee 6, 12489 Berlin, Germany

M. G. Raizen

Department of Physics, University of Texas, Austin, Texas 78712

The interference pattern of the resonance fluorescence from a $J=1/2$ to $J=1/2$ transition of two identical atoms confined in a three-dimensional harmonic potential is calculated. The thermal motion of the atoms is included. Agreement is obtained with experiments [U. Eichmann *et al.*, Phys. Rev. Lett. **70**, 2359 (1993)]. Contrary to some theoretical predictions, but in agreement with the present calculations, a fringe visibility greater than 50% can be observed with polarization-selective detection. The dependence of the fringe visibility on polarization has a simple interpretation, based on whether or not it is possible in principle to determine which atom emitted the photon. [S1050-2947(98)01606-0]

I. INTRODUCTION

Many variants of two-slit interference experiments, often ''thought experiments,'' have been used to illustrate fundamental principles of quantum mechanics. Recently, Eichmann *et al.* [1] have observed interference fringes in the resonance fluorescence of two trapped ions, analogous to those seen in Young's two-slit experiment. Of particular interest was the fact that the interference fringes appeared when it was impossible in principle to determine which ion scattered the photon and disappeared when it was possible to do so. This is in agreement with Bohr's principle of complementarity, which requires that the wave nature of the photon (the interference fringes) cannot be observed under the same conditions as its particle nature (the possibility of assigning to the photon a trajectory that intersects just one of the ions). In contrast to many thought experiments [2], the disappearance of the fringes when the path of the particle can be determined cannot be understood in terms of random classical momentum kicks. The experiment contains features from some thought experiments of Scully and Drühl [3], regarding the interference of light scattered by two multilevel atoms.

Recently, controversy has arisen over the mechanism by which complementarity is enforced in a two-slit interference experiment. Some claim that the destruction of interference by a determination of the particle's path is *always* due to a random momentum transfer necessitated by the indeterminacy relations [4–6]. Others claim that the mere *existence* of the path information can be sufficient to destroy the interference [7]. Englert *et al.* claim that the experiment of Eichmann *et al.* supports the second position [8].

Published calculations explain some aspects of the observations of Eichmann *et al.* [9–13]. However, none of those calculations include all of the factors required to make a comparison with the experimental data. Here we calculate the scattering cross section for arbitrary directions and polarizations of the incident and outgoing light. While the results

were used in the analysis of the data in Ref. [1], the details of the calculations were not given. The main limitation of the calculation is the use of perturbation theory, so that it is valid only for low light intensities. However, it includes the effect of thermal motion more precisely than has been done elsewhere, taking into account the actual normal modes of the system. Also, the actual experimental geometry is fully taken into account, which is not always the case in the other calculations.

Finally, we clarify the sense in which the loss of the fringe visibility [defined as $(I_{max}-I_{min})/(I_{max}+I_{min})$] for certain detected polarizations is due to the existence of ''which path'' information in the ions. This is an application of the fundamental quantum principle that transition amplitudes are to be added before squaring if and only if they connect the same initial and final states.

II. EXPERIMENT

The experimental apparatus has been described previously [1,14]. Figure 1 shows the geometry. Two ^{198}Hg$^+$ ions were confined in a linear Paul (rf) trap by a combination of static and rf electric fields. The ions were laser cooled to temperatures of a few mK with a beam of linearly polarized, continuous-wave light, nearly resonant with the 194-nm transition from the ground $6s\,^2S_{1/2}$ level to the $6p\,^2P_{1/2}$ level. The laser beam diameter was about 50 μm and the power was 50 μW or less. The same beam was the coherent source for Young's interference. Cooling in the trap resulted in strong localization of the ions, which was essential for observation of interference fringes. The trap potentials were arranged so that a pair of ions would be oriented along the symmetry (Z) axis of the trap. The incoming photons, with wave vector $\mathbf{k}_{in}$ and polarization vector $\hat{\boldsymbol{\epsilon}}_{in}$, made an angle Θ of 62° with respect to the Z axis. The X axis is oriented so that the X-Z plane contains $\mathbf{k}_{in}$. Light emitted by the ions was collimated by a lens and directed to the surface of an
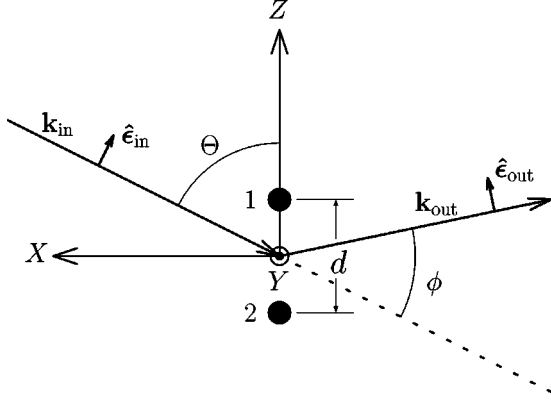
FIG. 1. Geometry of Young's interference experiment, projected onto the X-Z plane. The equilibrium positions of the two ions, represented by the filled circles, lie along the Z axis. The wave vector $\mathbf{k}_{\text{in}}$ of the incoming photon is in the X-Z plane, making an angle Θ with the Z axis. The Y axis is out of the plane of the figure. The projection of the wave vector $\mathbf{k}_{\text{out}}$ onto the X-Z plane makes an angle ϕ with $\mathbf{k}_{\text{in}}$. The angle that $\mathbf{k}_{\text{out}}$ deviates from the X-Z plane in the $+Y$ direction is Φ (not shown). The polarization vectors of the incoming and outgoing photons are $\hat{\boldsymbol{\epsilon}}_{\text{in}}$ and $\hat{\boldsymbol{\epsilon}}_{\text{out}}$.

imaging photodetector, which was used to observe the fringes. The wave vector and polarization of an outgoing photon are $\mathbf{k}_{\text{out}}$ and $\hat{\boldsymbol{\epsilon}}_{\text{out}}$. The projection of $\mathbf{k}_{\text{out}}$ onto the X-Z plane makes an angle ϕ with respect to $\mathbf{k}_{\text{in}}$. The deviation of $\mathbf{k}_{\text{out}}$ from the X-Z plane in the $+Y$ direction is Φ (not shown in Fig. 1). The sensitive area of the photodetector included a range of ϕ from about $15°$ to $45°$ and a range of Φ from about $-15°$ to $+15°$. For polarization-selective detection, a glass plate oriented at Brewster's angle was placed in the detection path so that nearly all of the light with $\hat{\boldsymbol{\epsilon}}_{\text{out}}$ in the X-Z plane was transmitted into the glass, while some of the light polarized along the Y axis was reflected to the imaging detector. The input polarization $\hat{\boldsymbol{\epsilon}}_{\text{in}}$ was varied. Another lens system formed a real image of the ions on a second imaging detector. This image was used to determine when there were precisely two ions in the trap.

III. TWO-ION HARMONIC-OSCILLATOR SYSTEM

In the pseudopotential approximation, the Hamiltonian for the translational motion of the two ions in the harmonic trap is

$$H_{\text{trans}} = \frac{\mathbf{P}_1^2}{2m} + \frac{\mathbf{P}_2^2}{2m} + V(\mathbf{R}_1) + V(\mathbf{R}_2) + \frac{e^2}{4\pi\epsilon_0 |\mathbf{R}_1 - \mathbf{R}_2|}, \tag{1}$$

where $\mathbf{R}_i$ and $\mathbf{P}_i$ are the position and momentum of the ith ion, e and m are the charge and mass of an ion, and

$$V(\mathbf{R}) \equiv \frac{1}{2}m\omega_R^2(X^2 + Y^2) + \frac{1}{2}m\omega_Z^2 Z^2 \tag{2}$$

is the potential energy of a single ion in the trap. In Eq. (2) we have made the approximation that the trap pseudopotential is cylindrically symmetric. Here $\mathbf{R} = (X,Y,Z)$, in the Cartesian coordinate system shown in Fig. 1. The classical
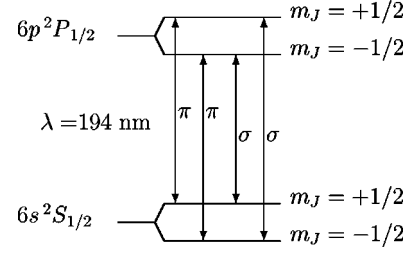

FIG. 2. Zeeman sublevels involved in the 194-nm, $6s\ ^2S_{1/2}$ to $6p\ ^2P_{1/2}$ transition of ^{198}Hg$^+$. The allowed π and σ transitions are labeled. The Zeeman splitting of the levels is exaggerated.

equilibrium positions of the ions, found by minimizing the total potential energy, are $\mathbf{R}_1^0 = (d/2)\hat{\mathbf{Z}}$ and $\mathbf{R}_2^0 = -(d/2)\hat{\mathbf{Z}}$, where $d = (e^2/2\pi\epsilon_0 m\omega_Z^2)^{1/3}$, and it is assumed that $\omega_R > \omega_Z$.

For small displacements $\mathbf{u}_1 = \mathbf{R}_1 - \mathbf{R}_1^0$ and $\mathbf{u}_2 = \mathbf{R}_2 - \mathbf{R}_2^0$ about the equilibrium positions, a harmonic approximation can be made. The Hamiltonian separates into terms involving either center-of-mass (c.m.) or relative coordinates and momenta defined by

$$\mathbf{u}^{\text{c.m.}} \equiv (\mathbf{u}_1 + \mathbf{u}_2)/2,$$

$$\mathbf{u}^{\text{rel}} \equiv (\mathbf{u}_1 - \mathbf{u}_2)/2,$$

$$\mathbf{P}^{\text{c.m.}} \equiv \mathbf{P}_1 + \mathbf{P}_2,$$

$$\mathbf{P}^{\text{rel}} \equiv \mathbf{P}_1 - \mathbf{P}_2. \tag{3}$$

The translational Hamiltonian, in the harmonic approximation, is

$$H_{\text{trans}} = \hbar\omega_Z(N_Z^{\text{c.m.}} + 1/2) + \hbar\omega_R(N_X^{\text{c.m.}} + N_Y^{\text{c.m.}} + 1)$$

$$+ \hbar\omega_S(N_Z^{\text{rel}} + 1/2) + \hbar\omega_T(N_X^{\text{rel}} + N_Y^{\text{rel}} + 1). \tag{4}$$

The number operators are defined in the usual way by $N_i^{\text{c.m.}} \equiv (a_i^{\text{c.m.}})^\dagger a_i^{\text{c.m.}}$ and $N_i^{\text{rel}} \equiv (a_i^{\text{rel}})^\dagger a_i^{\text{rel}}$ for $i = X,Y,Z$. The annihilation operators are defined in the usual way, for example,

$$a_Z^{\text{c.m.}} \equiv \sqrt{\frac{m\omega_Z}{\hbar}} u_Z^{\text{c.m.}} + \frac{i}{\sqrt{4\hbar m\omega_Z}} P_Z^{\text{c.m.}}. \tag{5}$$

The three center-of-mass modes have the same frequencies as those of a single ion in the trap: ω_Z and ω_R. The three relative modes include a symmetric stretch mode along the Z direction at frequency $\omega_S = \sqrt{3}\omega_Z$ and two tilting or rocking modes along the X and Y directions at frequency $\omega_T = (\omega_R^2 - \omega_Z^2)^{1/2}$. The eigenstates of H_{trans} are the simultaneous eigenstates of the set of number operators $|n_X^{\text{c.m.}}, n_Y^{\text{c.m.}}, n_Z^{\text{c.m.}}, n_X^{\text{rel}}, n_Y^{\text{rel}}, n_Z^{\text{rel}}\rangle$ with eigenvalues $\hbar[\omega_Z(n_Z^{\text{c.m.}} + 1/2) + \omega_R(n_X^{\text{c.m.}} + n_Y^{\text{c.m.}} + 1) + \omega_S(n_Z^{\text{rel}} + 1/2) + \omega_T(n_X^{\text{rel}} + n_Y^{\text{rel}} + 1)]$.

IV. ATOMIC LEVEL STRUCTURE

Figure 2 shows the magnetic sublevels involved in the $6s\ ^2S_{1/2}$ to $6p\ ^2P_{1/2}$ transition. These levels form an approximately closed system since the probability that the $6p\ ^2P_{1/2}$

level radiatively decays to the $5d^96s^2\,^2D_{3/2}$ level is only 1.4×10^{-7} [15]. The rest of the time it returns to the ground $6s\,^2S_{1/2}$ level. The $5d^96s^2\,^2D_{3/2}$ level has a lifetime of 9-ms and decays with about equal probability to the ground level or to the $5d^96s^2\,^2D_{5/2}$, which has a lifetime of 86-ms and decays only to the ground level.

Since the static magnetic field is small, we are free to define the quantization axis of the ions to be along the electric polarization vector $\hat{\boldsymbol{\epsilon}}_{\rm in}$ of the incident light. If the static magnetic field is along some other direction, then the Zeeman sublevels defined according to the electric polarization vector are not stationary states. This does not change the analysis as long as the Zeeman precession frequency is much less than the inverse of the scattering time, which is approximately equal to the $6p\,^2P_{1/2}$ state lifetime (2.3 ns). In the experiments described here, the magnetic field was small enough that this was always the case.

Figure 3 shows a Cartesian coordinate system having its z axis oriented along $\hat{\boldsymbol{\epsilon}}_{\rm in}$. The x axis is parallel to $\mathbf{k}_{\rm in}$. The y axis is defined so that (x,y,z) forms a right-handed coordinate system. This coordinate system is more useful than the trap-oriented (X,Y,Z) coordinate system of Fig. 1 for describing the angular distribution of the scattered light.

V. SCATTERING CROSS SECTION

Consider the process in which two ions, initially in their ground electronic states, absorb a photon having a wave vector $\mathbf{k}_{\rm in}$ and polarization $\hat{\boldsymbol{\epsilon}}_{\rm in}$, emit a photon having a wave vector $\mathbf{k}_{\rm out}$ and polarization $\hat{\boldsymbol{\epsilon}}_{\rm out}$ and are left in their ground electronic states. The ions may change their Zeeman sublevels during the process. Also, the motional state of the two ions may change.

The electric-dipole Hamiltonian that causes the transitions is

$$H_{\rm ED}=-\mathbf{D}_1\cdot\mathbf{E}(\mathbf{R}_1,t)-\mathbf{D}_2\cdot\mathbf{E}(\mathbf{R}_2,t), \qquad (6)$$

where $\mathbf{D}_1$ and $\mathbf{D}_2$ are the electric-dipole moment operators

FIG. 3. Coordinate system for description of the direction and polarization of the outgoing photon. The z axis is parallel to $\hat{\boldsymbol{\epsilon}}_{\rm in}$ and the x axis is parallel to $\mathbf{k}_{\rm in}$. The polarization vector $\hat{\boldsymbol{\epsilon}}_{\pi}$ lies in the plane containing $\hat{\boldsymbol{\epsilon}}_{\rm in}$ and $\mathbf{k}_{\rm out}$, while $\hat{\boldsymbol{\epsilon}}_{\sigma}$ is perpendicular to that plane.

for ions 1 and 2 and $\mathbf{E}(\mathbf{R},t)$ is the electric field, consisting of a classical part, representing the incident laser beam, and the quantized free field operator

$$\mathbf{E}(\mathbf{R},t)=\hat{\boldsymbol{\epsilon}}_{\rm in}{\rm Re}\mathcal{E}_0e^{i\mathbf{k}_{\rm in}\cdot\mathbf{R}-i\omega_{\rm in}t}$$

$$+\sum_s i\sqrt{\frac{\hbar\omega_s}{2\epsilon_0 V}}[a_s\hat{\boldsymbol{\epsilon}}_s e^{i\mathbf{k}_s\cdot\mathbf{R}}-a_s^\dagger\hat{\boldsymbol{\epsilon}}_s e^{-i\mathbf{k}_s\cdot\mathbf{R}}], \quad (7)$$

where Re denotes the real part, $\mathcal{E}_0$ is the amplitude of the laser electric field, a_s is the annihilation operator for a photon of wave vector $\mathbf{k}_s$, frequency ω_s, and polarization $\boldsymbol{\epsilon}_s$, and V is the quantization volume.

The electric-dipole Hamiltonian, in second-order perturbation theory, gives the cross section for the two ions to scatter a photon in a particular direction:

$$\frac{d\sigma_i}{d\Omega_{\rm out}}=\sum_f C_1\left|\sum_j\frac{\langle\Psi_f|(\mathbf{D}_1\cdot\hat{\boldsymbol{\epsilon}}_{\rm out})e^{-i\mathbf{k}_{\rm out}\cdot\mathbf{R}_1}|\Psi_j\rangle\langle\Psi_j|(\mathbf{D}_1\cdot\hat{\boldsymbol{\epsilon}}_{\rm in})e^{i\mathbf{k}_{\rm in}\cdot\mathbf{R}_1}|\Psi_i\rangle}{\omega_0-\omega_{\rm in}+(E_j-E_i)/\hbar-i\gamma/2}\right.$$

$$\left.+\sum_j\frac{\langle\Psi_f|(\mathbf{D}_2\cdot\hat{\boldsymbol{\epsilon}}_{\rm out})e^{-i\mathbf{k}_{\rm out}\cdot\mathbf{R}_2}|\Psi_j\rangle\langle\Psi_j|(\mathbf{D}_2\cdot\hat{\boldsymbol{\epsilon}}_{\rm in})e^{i\mathbf{k}_{\rm in}\cdot\mathbf{R}_2}|\Psi_i\rangle}{\omega_0-\omega_{\rm in}+(E_j-E_i)/\hbar-i\gamma/2}\right|^2, \qquad (8)$$

where $\omega_{\rm in}=c|\mathbf{k}_{\rm in}|$, $\omega_{\rm out}=c|\mathbf{k}_{\rm out}|$, $\hbar\omega_0$ is the separation between the ground and excited electronic states of an ion, γ is the decay rate of the excited state, and $C_1\equiv\omega_{\rm out}^3/16\pi^2c^4\hbar^2\epsilon_0^2$. The initial, final, and intermediate states describing the electronic and motional degrees of freedom of the system are $|\Psi_i\rangle$, $|\Psi_f\rangle$, and $|\Psi_j\rangle$. The energies E_i, E_f, and E_j are the motional energies of the ions in the initial, final, and intermediate states. They depend on the values of the six harmonic-oscillator quantum numbers,
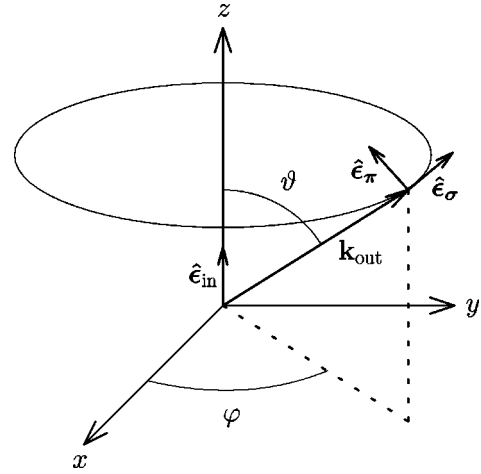
which we denote by $\{n_{\rm HO}\}$. Because of energy conservation, the frequency of the outgoing photon depends on the final state

$$\omega_{\rm out}=\omega_{\rm in}+(E_i-E_f)/\hbar. \qquad (9)$$

Thus the scattered light has a discrete frequency spectrum and the different components could, in principle, be detected separately. In Eq. (8) all frequency components are summed,

which is appropriate if the detection is frequency insensitive. The laser frequency is assumed to be nearly resonant with an optical transition in the ion, so that only one intermediate electronic state has to be included in the sums and we can neglect the counterrotating terms. We ignore dipole-dipole interactions between the ions because they were separated by many wavelengths in the experiment. Here we specialize to the case of an ion that has no nuclear spin and has a $^2S_{1/2}$ ground state and a $^2P_{1/2}$ excited state, like the ^{198}Hg$^+$ ions used in Ref. [1]. We denote a state in which ion 1 is in the $^2S_{1/2}$, $m_J = +1/2$ state, ion 2 is in the $^2P_{1/2}$, $m_J = -1/2$ state, and has the harmonic-oscillator quantum numbers $\{n_{HO}\}$ by

$$|\Psi\rangle = |(^2S_{1/2}, +1/2)_1(^2P_{1/2}, -1/2)_2\{n_{HO}\}\rangle. \quad (10)$$

There are four possible sets of initial m_J quantum numbers for the two ions and four possible final sets. There are two basic kinds of scattering processes, those that preserve the m_J quantum numbers of the ions and those that change m_J of one ion. We treat these cases separately. The form of Eq. (8) excludes the possibility of both ions changing their m_J quantum numbers.

A. Both m_J quantum numbers remain the same (π case)

In order to be definite, we set $m_J = +1/2$ for both ions, both before and after the scattering, that is,

$$|\Psi_i\rangle = |(^2S_{1/2}, +1/2)_1(^2S_{1/2}, +1/2)_2\{n_{HO}\}_i\rangle, \quad (11)$$

$$|\Psi_f\rangle = |(^2S_{1/2}, +1/2)_1(^2S_{1/2}, +1/2)_2\{n_{HO}\}_f\rangle. \quad (12)$$

We call this the π case because it involves only π transitions, that is, transitions that leave m_J unchanged. Because of the electric-dipole selection rules, the only intermediate states that contribute nonzero terms are of the form

$$|\Psi_j\rangle = |(^2P_{1/2}, +1/2)_1(^2S_{1/2}, +1/2)_2\{n_{HO}\}_j\rangle \quad (13)$$

for the first sum and

$$|\Psi_j\rangle = |(^2S_{1/2}, +1/2)_1(^2P_{1/2}, +1/2)_2\{n_{HO}\}_j\rangle \quad (14)$$

for the second sum. The matrix elements connecting the initial states to the intermediate states are

$$\langle\Psi_j|(\mathbf{D}_p \cdot \hat{\boldsymbol{\epsilon}}_{in})e^{i\mathbf{k}_{in} \cdot \mathbf{R}_p}|\Psi_i\rangle = \langle(^2P_{1/2}, +1/2)_p|D_{pz}|(^2S_{1/2}, +1/2)_p\rangle\langle\{n_{HO}\}_j|e^{i\mathbf{k}_{in} \cdot \mathbf{R}_p}|\{n_{HO}\}_i\rangle$$

$$= \frac{1}{\sqrt{6}}(^2P_{1/2}\|D^{(1)}\|^2S_{1/2})\langle\{n_{HO}\}_j|e^{i\mathbf{k}_{in} \cdot \mathbf{R}_p}|\{n_{HO}\}_i\rangle, \quad (15)$$

where $p = 1$ or 2, D_{pz} is the z component of the $\mathbf{D}_p$ operator, and $(^2P_{1/2}\|D^{(1)}\|^2S_{1/2})$ is the reduced matrix element of the dipole moment operator (the same for both ions).

The angular distribution of the outgoing photon is contained in the matrix elements connecting the intermediate states to the final states. The unit propagation vector for the outgoing photon is

$$\hat{k}_{out} = (\sin\vartheta\cos\varphi, \sin\vartheta\sin\varphi, \cos\vartheta), \quad (16)$$

where ϑ and φ are spherical polar angles with respect to the (x,y,z) coordinate system of Fig. 3. The polarization vector $\hat{\boldsymbol{\epsilon}}_{out}$ must be perpendicular to $\hat{k}_{out}$. We define two mutually orthogonal unit polarization vectors, both perpendicular to $\hat{k}_{out}$, by

$$\hat{\boldsymbol{\epsilon}}_\pi = (-\cos\vartheta\cos\varphi, -\cos\vartheta\sin\varphi, \sin\vartheta) \quad (17)$$

and

$$\hat{\boldsymbol{\epsilon}}_\sigma = (-\sin\varphi, \cos\varphi, 0). \quad (18)$$

Since only the z components of $\mathbf{D}_1$ and $\mathbf{D}_2$ contribute to the matrix elements connecting the intermediate and final states for this case, light with polarization vector $\hat{\boldsymbol{\epsilon}}_\sigma$ cannot be emitted.

With the choice of $\hat{\boldsymbol{\epsilon}}_{out} = \hat{\boldsymbol{\epsilon}}_\pi$, the matrix elements connecting the intermediate states to the final states are

$$\langle\Psi_f|(\mathbf{D}_p \cdot \hat{\boldsymbol{\epsilon}}_\pi)e^{-i\mathbf{k}_{out} \cdot \mathbf{R}_p}|\Psi_j\rangle = \sin\vartheta\langle(^2S_{1/2}, +1/2)_p|D_{pz}|(^2P_{1/2}, +1/2)_p\rangle\langle\{n_{HO}\}_f|e^{-i\mathbf{k}_{out} \cdot \mathbf{R}_p}|\{n_{HO}\}_j\rangle$$

$$= \frac{\sin\vartheta}{\sqrt{6}}(^2S_{1/2}\|D^{(1)}\|^2P_{1/2})\langle\{n_{HO}\}_f|e^{-i\mathbf{k}_{out} \cdot \mathbf{R}_p}|\{n_{HO}\}_j\rangle. \quad (19)$$

Equation (8) for the cross section becomes

$$\frac{d\sigma^{(1)}}{d\Omega_{\text{out}}} = \frac{\sin^2\vartheta}{36}|(^2S_{1/2}\|D^{(1)}\|^2P_{1/2})|^4\sum_f C_1\left|\sum_j \frac{\langle\{n_{\text{HO}}\}_f|e^{-i\mathbf{k}_{\text{out}}\cdot\mathbf{R}_1}|\{n_{\text{HO}}\}_j\rangle\langle\{n_{\text{HO}}\}_j|e^{i\mathbf{k}_{\text{in}}\cdot\mathbf{R}_1}|\{n_{\text{HO}}\}_i\rangle}{\omega_0 - \omega_{\text{in}} + (E_j - E_i)/\hbar - i\gamma/2}\right.$$

$$\left. + \sum_j \frac{\langle\{n_{\text{HO}}\}_f|e^{-i\mathbf{k}_{\text{out}}\cdot\mathbf{R}_2}|\{n_{\text{HO}}\}_j\rangle\langle\{n_{\text{HO}}\}_j|e^{i\mathbf{k}_{\text{in}}\cdot\mathbf{R}_2}|\{n_{\text{HO}}\}_i\rangle}{\omega_0 - \omega_{\text{in}} + (E_j - E_i)/\hbar - i\gamma/2}\right|^2. \tag{20}$$

The (1) superscript on the cross section is to label it as the π case. The same result would have been obtained for any of the other three possible sets of initial m_J quantum numbers, so this is the general result for the case in which the m_J values do not change. The presence of two terms in Eq. (20), which are added and then squared, is the source of Young's interference fringes. These two terms can be identified with the two possible paths for the photon, each intersecting one of the two ions.

The sums over intermediate harmonic-oscillator states can be done by closure if the energy denominators are constant. While they are not constant, because $E_j - E_i$ varies, it can be

shown (see, for example, Ref. [16]) that the main contributions to the sum come from terms where $|E_j - E_i|$ is less than or on the order of $\sqrt{RE_i}$, where R is the photon recoil energy $(\hbar k_{\text{out}})^2/2m$. For the Hg$^+$ 194.2-nm transition, $R = h \times 26.7$ kHz. For Doppler cooling, E_i will be on the order of $\hbar\gamma$, where, for this transition, $\hbar\gamma = h \times 70$ MHz. Thus the rms value of $E_j - E_i$ will be on the order of $h \times 1.4$ MHz, which is much less than $\hbar\gamma/2$. Therefore, while the denominators are not strictly constant, they are nearly constant for the terms that contribute significantly to the sums.

If we neglect $(E_j - E_i)/\hbar$ compared to $\gamma/2$ and use closure to evaluate the sums, Eq. (20) simplifies to

$$\frac{d\sigma^{(1)}}{d\Omega_{\text{out}}} = \frac{\sin^2\vartheta}{36}\frac{|(^2S_{1/2}\|D^{(1)}\|^2P_{1/2})|^4}{(\omega_0 - \omega_{\text{in}})^2 + \gamma^2/4}\sum_f C_1|\langle\{n_{\text{HO}}\}_f|e^{-i\mathbf{k}_{\text{out}}\cdot\mathbf{R}_1}e^{i\mathbf{k}_{\text{in}}\cdot\mathbf{R}_1}|\{n_{\text{HO}}\}_i\rangle + \langle\{n_{\text{HO}}\}_f|e^{-i\mathbf{k}_{\text{out}}\cdot\mathbf{R}_2}e^{i\mathbf{k}_{\text{in}}\cdot\mathbf{R}_2}|\{n_{\text{HO}}\}_i\rangle|^2$$

$$= \frac{\sin^2\vartheta}{36}\frac{(^2S_{1/2}\|D^{(1)}\|^2P_{1/2})|^4}{(\omega_0 - \omega_{\text{in}})^2 + \gamma^2/4}\sum_f C_1|\langle\{n_{\text{HO}}\}_f|e^{-i\mathbf{q}\cdot\mathbf{R}_1}|\{n_{\text{HO}}\}_i\rangle + \langle\{n_{\text{HO}}\}_f|e^{-i\mathbf{q}\cdot\mathbf{R}_2}|\{n_{\text{HO}}\}_i\rangle|^2$$

$$= \frac{\sin^2\vartheta}{36}\frac{|(^2S_{1/2}\|D^{(1)}\|^2P_{1/2})|^4}{(\omega_0 - \omega_{\text{in}})^2 + \gamma^2/4}\sum_f C_1|\langle\{n_{\text{HO}}\}_f|e^{-i\mathbf{q}\cdot\mathbf{R}_1} + e^{-i\mathbf{q}\cdot\mathbf{R}_2}|\{n_{\text{HO}}\}_i\rangle|^2, \tag{21}$$

where $\mathbf{q} \equiv \mathbf{k}_{\text{out}} - \mathbf{k}_{\text{in}}$. Since the branching ratio for decay of the excited $^2P_{1/2}$ states to the ground $^2S_{1/2}$ states is nearly 100%, the spontaneous decay rate γ is

$$\gamma = \frac{\omega_0^3}{6\pi\epsilon_0\hbar c^3}|(^2S_{1/2}\|D^{(1)}\|^2P_{1/2})|^2. \tag{22}$$

Equation (21) for the cross section becomes

$$\frac{d\sigma^{(1)}}{d\Omega_{\text{out}}} = \frac{\sin^2\vartheta}{8\pi}\sigma_0\mathcal{L}(\omega_{\text{in}} - \omega_0)$$

$$\times\sum_f |\langle\{n_{\text{HO}}\}_f|e^{-i\mathbf{q}\cdot\mathbf{R}_1} + e^{-i\mathbf{q}\cdot\mathbf{R}_2}|\{n_{\text{HO}}\}_i\rangle|^2, \tag{23}$$

where $\sigma_0 = \lambda_0^2/2\pi$ is the resonance cross section, $\lambda_0 = 2\pi c/\omega_0$ is the resonance wavelength, and $\mathcal{L}(\omega_{\text{in}} - \omega_0)$ is a Lorentzian of unit height and width γ:

$$\mathcal{L}(\omega_{\text{in}} - \omega_0) \equiv \frac{(\gamma/2)^2}{(\omega_{\text{in}} - \omega_0)^2 + (\gamma/2)^2}. \tag{24}$$

In deriving Eq. (23) we have assumed that $\omega_0/\omega_{\text{out}} \approx 1$. The sum over final harmonic-oscillator states can be done by closure:

$$\frac{d\sigma^{(1)}}{d\Omega_{\text{out}}} = \frac{\sin^2\vartheta}{8\pi}\sigma_0\mathcal{L}(\omega_{\text{in}} - \omega_0)\langle\{n_{\text{HO}}\}_i|(e^{i\mathbf{q}\cdot\mathbf{R}_1} + e^{i\mathbf{q}\cdot\mathbf{R}_2})$$

$$\times(e^{-i\mathbf{q}\cdot\mathbf{R}_1} + e^{-i\mathbf{q}\cdot\mathbf{R}_2})|\{n_{\text{HO}}\}_i\rangle$$

$$= \frac{\sin^2\vartheta}{8\pi}\sigma_0\mathcal{L}(\omega_{\text{in}} - \omega_0)\langle\{n_{\text{HO}}\}_i|2 + e^{i\mathbf{q}\cdot(\mathbf{R}_1 - \mathbf{R}_2)}$$

$$+ e^{-i\mathbf{q}\cdot(\mathbf{R}_1 - \mathbf{R}_2)}|\{n_{\text{HO}}\}_i\rangle. \tag{25}$$

The exponentials can be combined in Eq. (25) because the components of $\mathbf{R}_1$ and $\mathbf{R}_2$ commute. The cross section can be written in terms of the equilibrium ion separation $\mathbf{d}$ and the displacement coordinates $\mathbf{u}_1$ and $\mathbf{u}_2$ as

$$\frac{d\sigma^{(1)}}{d\Omega_{\text{out}}} = \frac{\sin^2\vartheta}{8\pi}\sigma_0\mathcal{L}(\omega_{\text{in}} - \omega_0)\langle\{n_{\text{HO}}\}_i|2 + e^{i\mathbf{q}\cdot(\mathbf{d} + \mathbf{u}_1 - \mathbf{u}_2)}$$

$$+ e^{-i\mathbf{q}\cdot(\mathbf{d} + \mathbf{u}_1 - \mathbf{u}_2)}|\{n_{\text{HO}}\}_i\rangle. \tag{26}$$

The exponential factors in Eq. (26) depend on the relative coordinates of the two ions and not on their center-of-mass coordinates.

In order to compare with the experiment, we compute the cross section averaged over a thermal distribution of $|\{n_{HO}\}_i\rangle$ initial states:

$$\left\langle \frac{d\sigma^{(1)}}{d\Omega_{out}} \right\rangle = \frac{\sin^2 \vartheta}{8\pi} \sigma_0 \mathcal{L}(\omega_{in} - \omega_0)[2 + e^{i\mathbf{q}\cdot\mathbf{d}}\langle e^{i\mathbf{q}\cdot(\mathbf{u}_1-\mathbf{u}_2)}\rangle$$
$$+ e^{-i\mathbf{q}\cdot\mathbf{d}}\langle e^{-i\mathbf{q}\cdot(\mathbf{u}_1-\mathbf{u}_2)}\rangle], \qquad (27)$$

where $\langle A \rangle$ denotes the thermal average of the operator A. For harmonic oscillators, the thermal averages have a simple form [17,18]

$$\langle e^{\pm i\mathbf{q}\cdot(\mathbf{u}_1-\mathbf{u}_2)}\rangle = e^{-\langle[\mathbf{q}\cdot(\mathbf{u}_1-\mathbf{u}_2)]^2\rangle/2}. \qquad (28)$$

While Refs. [17,18] assume a common temperature for all of the harmonic-oscillator modes, Eq. (28) is still valid if different modes have different temperatures. Different modes are laser cooled at different rates depending on the direction of the laser beam. Hence the modes have different temperatures unless the energy transfer rate between them is fast [19]. The thermally averaged cross section is

$$\left\langle \frac{d\sigma^{(1)}}{d\Omega_{out}} \right\rangle = \frac{\sin^2 \vartheta}{4\pi} \sigma_0 \mathcal{L}(\omega_{in} - \omega_0)$$
$$\times [1 + \cos(\mathbf{q}\cdot\mathbf{d})e^{-\langle[\mathbf{q}\cdot(\mathbf{u}_1-\mathbf{u}_2)]^2\rangle/2}], \qquad (29)$$

which is equivalent to Eq. (1) of Ref. [1], except that it includes the $\sin^2 \vartheta$ angular dependence. The interference fringe visibility is given by the exponential factor multiplying $\cos(\mathbf{q}\cdot\mathbf{d})$. This factor decreases with increasing temperature and is analogous to the Debye-Waller factor for x-ray scattering from a crystal. It can be rewritten as

$$e^{-\langle[\mathbf{q}\cdot(\mathbf{u}_1-\mathbf{u}_2)]^2\rangle/2} = \exp\left[-\frac{\hbar q_X^2}{m\omega_T}\left(\langle N_X^{rel}\rangle + \frac{1}{2}\right) - \frac{\hbar q_Y^2}{m\omega_T}\left(\langle N_Y^{rel}\rangle + \frac{1}{2}\right) - \frac{\hbar q_Z^2}{m\omega_S}\left(\langle N_Z^{rel}\rangle + \frac{1}{2}\right) \right]$$

$$= \exp\left[-\frac{\hbar q_X^2}{2m\omega_T}\coth\left(\frac{\hbar\omega_T}{2k_B T_X^{rel}}\right) - \frac{\hbar q_Y^2}{2m\omega_T}\coth\left(\frac{\hbar\omega_T}{2k_B T_Y^{rel}}\right) - \frac{\hbar q_Z^2}{2m\omega_S}\coth\left(\frac{\hbar\omega_S}{2k_B T_Z^{rel}}\right) \right]$$

$$\approx \exp\left(-\frac{q_X^2 k_B T_X^{rel}}{m\omega_T^2} - \frac{q_Y^2 k_B T_Y^{rel}}{m\omega_T^2} - \frac{q_Z^2 k_B T_Z^{rel}}{m\omega_S^2} \right), \qquad (30)$$

where T_Z^{rel} is the temperature of the u_Z^{rel} mode, etc., and the approximation in the last line is valid when the mean harmonic-oscillator quantum numbers are large. In the limit of small thermal motion or small $|\mathbf{q}|$ (near-forward scattering), the visibility can approach 100% (with polarized detection), in agreement with Ref. [13], but in contradiction to Ref. [11], where it was claimed that the visibility could not exceed 50%.

B. One m_J quantum number changes (σ case)

Here we consider the case in which one of the ions changes its m_J quantum number in the scattering process. We call this the σ case since it involves a σ transition, that is, a transition that changes m_J by ± 1 in one of the ions. There are eight cases since there are four possible initial states and two ions that could change quantum numbers.

In order to be definite, we pick the case where $m_J = +1/2$ for both ions before the scattering and ion 1 changes to $m_J = -1/2$ after the scattering, that is,

$$|\Psi_i\rangle = |(^2S_{1/2}, +1/2)_1(^2S_{1/2}, +1/2)_2\{n_{HO}\}_i\rangle, \qquad (31)$$

$$|\Psi_f\rangle = |(^2S_{1/2}, -1/2)_1(^2S_{1/2}, +1/2)_2\{n_{HO}\}_f\rangle. \qquad (32)$$

Only the first sum over j in Eq. (8) contributes since only it contains $\mathbf{D}_1$, the dipole moment that leads to the change in m_J of ion 1.

As in the previous case, the only intermediate states that contribute nonzero terms are of the form

$$|\Psi_j\rangle = |(^2P_{1/2}, +1/2)_1(^2S_{1/2}, +1/2)_2\{n_{HO}\}_j\rangle. \qquad (33)$$

The matrix elements connecting the initial states to the intermediate states are

$$\langle \Psi_j|(\mathbf{D}_1 \cdot \hat{\boldsymbol{\epsilon}}_{in})e^{i\mathbf{k}_{in}\cdot\mathbf{R}_1}|\Psi_i\rangle$$
$$= \langle(^2P_{1/2}, +1/2)_1|D_{1z}|(^2S_{1/2}, +1/2)_1\rangle$$
$$\times \langle\{n_{HO}\}_j|e^{i\mathbf{k}_{in}\cdot\mathbf{R}_1}|\{n_{HO}\}_i\rangle$$
$$= \frac{1}{\sqrt{6}}(^2P_{1/2}\|D^{(1)}\|^2S_{1/2})\langle\{n_{HO}\}_j|e^{i\mathbf{k}_{in}\cdot\mathbf{R}_1}|\{n_{HO}\}_i\rangle. \qquad (34)$$

In the $\vartheta = \pi/2$ plane, only the polarization corresponding to $\hat{\boldsymbol{\epsilon}}_\sigma$ is emitted, but, in general, light with both $\hat{\boldsymbol{\epsilon}}_\sigma$ and $\hat{\boldsymbol{\epsilon}}_\pi$ contributes to the scattered intensity. We consider these two cases separately.

For $\hat{\boldsymbol{\epsilon}}_{out} = \hat{\boldsymbol{\epsilon}}_\sigma$, the matrix elements connecting the intermediate states to the final states are

$$\langle\Psi_f|(\mathbf{D}_1\cdot\hat{\boldsymbol{\epsilon}}_\sigma)e^{-i\mathbf{k}_{\text{out}}\cdot\mathbf{R}_1}|\Psi_j\rangle$$

$$=\frac{-ie^{i\varphi}}{\sqrt{2}}\langle(^2S_{1/2},-1/2)_1|D_{1-1}^{(1)}|(^2P_{1/2},+1/2)_1\rangle$$

$$\times\langle\{n_{\text{HO}}\}_f|e^{-i\mathbf{k}_{\text{out}}\cdot\mathbf{R}_1}|\{n_{\text{HO}}\}_j\rangle$$

$$=\frac{-ie^{i\varphi}}{\sqrt{6}}(^2S_{1/2}\|D^{(1)}\|^2P_{1/2})\langle\{n_{\text{HO}}\}_f|e^{-i\mathbf{k}_{\text{out}}\cdot\mathbf{R}_1}|\{n_{\text{HO}}\}_j\rangle,$$

$$(35)$$

where $D_{p-1}^{(1)}$ is the $(1,-1)$ spherical tensor component of the dipole moment operator for ion p. The rest of the calculation

---

$$\langle\Psi_f|(\mathbf{D}_1\cdot\hat{\boldsymbol{\epsilon}}_\pi)e^{-i\mathbf{k}_{\text{out}}\cdot\mathbf{R}_1}|\Psi_j\rangle=\frac{-\cos\vartheta e^{i\varphi}}{\sqrt{2}}\langle(^2S_{1/2},-1/2)_1|D_{1-1}^{(1)}|(^2P_{1/2},+1/2)_1\rangle\langle\{n_{\text{HO}}\}_f|e^{-i\mathbf{k}_{\text{out}}\cdot\mathbf{R}_1}|\{n_{\text{HO}}\}_j\rangle$$

$$=\frac{-\cos\vartheta e^{i\varphi}}{\sqrt{6}}(^2S_{1/2}\|D^{(1)}\|^2P_{1/2})\langle\{n_{\text{HO}}\}_f|e^{-i\mathbf{k}_{\text{out}}\cdot\mathbf{R}_1}|\{n_{\text{HO}}\}_j\rangle. \qquad (37)$$

The final result is

$$\left\langle\frac{d\sigma^{(3)}}{d\Omega_{\text{out}}}\right\rangle=\frac{\cos^2\vartheta}{8\pi}\sigma_0\mathcal{L}(\omega_{\text{in}}-\omega_0), \qquad (38)$$

which shows no interference fringes. The same result would have been obtained for any of the other initial states.

For the σ case, Young's interference fringes are not observed because only one of the two terms inside the absolute value bars in Eq. (8) is nonzero. There is only one path for the photon, intersecting the ion whose state is changed in the scattering process.

C. Total cross section with or without polarization-selective detection

In Ref. [1] a linear polarizer was sometimes placed before the photon detector. For experimental convenience, the orientation of this polarizer was fixed, while the input polarization could be varied. To obtain the total cross section describing a given experimental situation, we sum over all final atomic states and average over all initial states. For polarization-insensitive detection, we also sum over the polarizations of the outgoing photon.

The cross section for polarization-insensitive detection is

$$\left\langle\frac{d\sigma^{\text{unpol}}}{d\Omega_{\text{out}}}\right\rangle=\left\langle\frac{d\sigma^{(1)}}{d\Omega_{\text{out}}}\right\rangle+2\left\langle\frac{d\sigma^{(2)}}{d\Omega_{\text{out}}}\right\rangle+2\left\langle\frac{d\sigma^{(3)}}{d\Omega_{\text{out}}}\right\rangle$$

$$=\frac{\sigma_0}{4\pi}\mathcal{L}(\omega_{\text{in}}-\omega_0)\{1+\cos^2\vartheta$$

$$+\sin^2\vartheta[1+\cos(\mathbf{q}\cdot\mathbf{d})e^{-\langle[\mathbf{q}\cdot(\mathbf{u}_1-\mathbf{u}_2)]^2\rangle/2}]\}. \qquad (39)$$

The fringe visibility in this case cannot exceed 50%.

is very similar to the π case. The final result, analogous to Eq. (29) for the π case, is

$$\left\langle\frac{d\sigma^{(2)}}{d\Omega_{\text{out}}}\right\rangle=\frac{1}{8\pi}\sigma_0\mathcal{L}(\omega_{\text{in}}-\omega_0), \qquad (36)$$

which is independent of $\hat{\mathbf{k}}_{\text{out}}$ and shows no interference fringes. The same result would have been obtained for any of the other three initial states since the absolute squares of the matrix elements are the same.

For $\hat{\boldsymbol{\epsilon}}_{\text{out}}=\hat{\boldsymbol{\epsilon}}_\pi$, the matrix elements connecting the intermediate states to the final states are

The cross section for detection of light with polarization $\hat{\boldsymbol{\epsilon}}_\pi$ is

$$\left\langle\frac{d\sigma^{(\pi)}}{d\Omega_{\text{out}}}\right\rangle=\left\langle\frac{d\sigma^{(1)}}{d\Omega_{\text{out}}}\right\rangle+2\left\langle\frac{d\sigma^{(3)}}{d\Omega_{\text{out}}}\right\rangle$$

$$=\frac{\sigma_0}{4\pi}\mathcal{L}(\omega_{\text{in}}-\omega_0)\{\cos^2\vartheta$$

$$+\sin^2\vartheta[1+\cos(\mathbf{q}\cdot\mathbf{d})e^{-\langle[\mathbf{q}\cdot(\mathbf{u}_1-\mathbf{u}_2)]^2\rangle/2}]\}. \qquad (40)$$

The fringe visibility in this case can approach 100% in the $\vartheta=\pi/2$ plane if the Debye-Waller factor is close to 1. The cross section for detection of light with polarization $\hat{\boldsymbol{\epsilon}}_\sigma$ is

$$\left\langle\frac{d\sigma^{(\sigma)}}{d\Omega_{\text{out}}}\right\rangle=2\left\langle\frac{d\sigma^{(2)}}{d\Omega_{\text{out}}}\right\rangle=\frac{\sigma_0}{4\pi}\mathcal{L}(\omega_{\text{in}}-\omega_0), \qquad (41)$$

which is totally isotropic and shows no fringes.

D. Which-path interpretation

The presence of interference fringes in the π case and their absence in the σ case have a simple explanation in terms of the possibility, in principle, of determining which of the two ions scattered the photon. Consider the sequence of transitions in Fig. 4(a), representing the π case. Each box represents the combined state of the two ions. Ion 1 is represented by the diagram on the left side of a box and ion 2 by that on the right. The ordering of energy levels is the same as in Fig. 2. For simplicity, we neglect the translational degrees of freedom, which lead to the appearance of the Debye-Waller factor in Eq. (29). The system begins in the state

$$|\Psi_i\rangle = |(^2S_{1/2},+1/2)_1(^2S_{1/2},-1/2)_2\rangle. \qquad (42)$$

One ion or the other absorbs a photon from the laser beam and undergoes a π transition to the excited state. That ion emits a photon and undergoes a π transition back to the ground state. The two paths, corresponding to either ion 1 or ion 2 scattering the photon, lead to the same final state. Therefore, the amplitudes for these two paths must be added and this leads to interference. Since the final states of the ion are the same as the initial states, it is not possible to determine which of the ions scattered the photon by examining their states.

Now consider the sequence of transitions in Fig. 4(b), representing the σ case. As in the previous case, one ion or the other absorbs a photon and undergoes a π transition to the excited state. However, in this case, that ion undergoes a σ transition when it emits a photon and changes its m_J quantum number. The final states differ, depending on which of the ions scattered the photon. Hence there is no interference between the two paths. It would be possible to tell which ion scattered the photon by examining the states of the ions before and after the scattering.

The preceding analysis is valid only in the limit of low laser intensity, so that the probability of both ions being excited at the same time is negligible and stimulated emission can be neglected. It is not necessary that the two ions be in the same quantum state for interference to occur, only that the final combined states for the two paths be indistinguishable. For definiteness, a particular initial state [Eq. (42)] was chosen. For each of the three other possible initial states, there is a process like Fig. 4(a) in which the ions scatter a photon and return to their original states and one like Fig. 4(b) in which one of them scatters a photon and changes its state. Processes of the former type lead to interference; those of the latter type do not.

VI. COMPARISON WITH EXPERIMENT

Figure 5 shows an image of the fringes observed for the π case in which $\hat{\boldsymbol{\epsilon}}_{\text{in}}$ was perpendicular to the X-Z plane and the detector was sensitive only to light polarized parallel to $\hat{\boldsymbol{\epsilon}}_{\text{in}}$. The dark spots are due to stray reflections of the laser beams. When $\hat{\boldsymbol{\epsilon}}_{\text{in}}$ was rotated by 90° without changing the polarizer in front of the detector (σ case), the image showed no fringes. The image data from a single ion, which shows no interference fringes, were used to correct the data of Fig. 5 for a slowly spatially varying detection efficiency. The data within the rectangle in Fig. 5 were summed along the vertical direction and divided by the detection-efficiency function.

The normalized data points are shown in Fig. 6 together with a least-squares fit. In this fit, as in Ref. [1], the temperatures of the stretch and tilt modes were assumed to have the ratio expected from theory [19],

$$T_Z^{\text{rel}}/T_X^{\text{rel}} = \{1 + [3\cos^2(\Theta)]^{-1}\}/\{1 + [3\sin^2(\Theta)]^{-1}\},$$
$$(43)$$

and both temperatures were allowed to vary together in the fit. The fringe visibility in the vicinity of the X-Z plane is insensitive to the temperature of the Y motion, which is cooled indirectly by coupling to the other modes. The mean

ion separation was calculated from knowledge of the trap parameters. The dependence of Eq. (29) on the out-of-plane angle Φ is small and Φ was set to 0 in the fit. The fitted value of T_X^{rel} was 1.08 ± 0.12 mK, or 0.92 ± 0.10 times the Doppler-cooling limit. The fringe visibility, extrapolated to $\phi = 0$, would be 100% if it followed Eq. (29). The fitted value for this parameter was $(71 \pm 4)\%$. The errors represent the standard deviations estimated from the fit. The maximum *observed* visibility at the minimum value of ϕ in Fig. 6 is approximately 60%.

There are several likely causes of the difference between the observed and predicted values of the fringe visibility. First, the theory was derived for the limit of low intensity. The saturation parameter was measured to be $s = 0.078 \pm 0.025$ (see the Appendix). By itself, this would reduce the maximum visibility to $(1+s)^{-1} \approx 93\%$ because the spectrum of the resonance fluorescence in this polarization contains an incoherent part [20]. Other likely causes of reduced visibility are unequal laser intensities at the two ions, imperfect polarizers, stray background light, and quantum jumps of one of the ions to a metastable state, leaving only one ion fluorescing. Each of these effects might reduce the visibility by a few percent.

VII. DISCUSSION

The fact that the resonance fluorescence from a two-level atom illuminated by weak, monochromatic light is coherent with the applied field was noted by Heitler [21]. The spectrum of the resonance fluorescence for arbitrary applied intensities was calculated by Mollow [22]. In the limit of low applied intensity, the spectrum is monochromatic and coherent with the applied field (a δ function). At higher intensities, the coherent component decreases in amplitude and a component not coherent with the applied field and having a width equal to the natural linewidth appears. At very high intensities, the coherent component continues to decrease in amplitude and the incoherent component splits into three separate Lorentzians. The existence of a coherent component in the resonance fluorescence of a single ion was confirmed directly by Höffges *et al.* by a heterodyne measurement [23].

Classically, we would expect the resonance fluorescence from two two-level atoms at fixed positions, excited by the same monochromatic field, to generate interference fringes having 100% visibility in the limit of low applied intensity since the radiated fields are coherent with each other. At higher applied intensities, the visibility should decrease since more of the resonance fluorescence intensity belongs to the incoherent component. Quantum treatments for two two-level atoms have been given by Richter [24] and by Kochan *et al.* [25], who predict a visibility equal to $(1+s)^{-1}$, where s is the saturation parameter defined in Ref. [26]. This is just the ratio of the intensity of the coherent component to the total resonance fluorescence intensity for a single atom.

Polder and Schuurmans [20] calculated the spectrum of the resonance fluorescence of a $J = 1/2$ to $J = 1/2$ transition for a single atom. The spectrum of the light having polarization $\hat{\boldsymbol{\epsilon}}_\pi$ is like that for a two-level atom. Hence interference fringes would be expected in the $\hat{\boldsymbol{\epsilon}}_\pi$-polarized resonance fluorescence from two such atoms for low applied intensity.
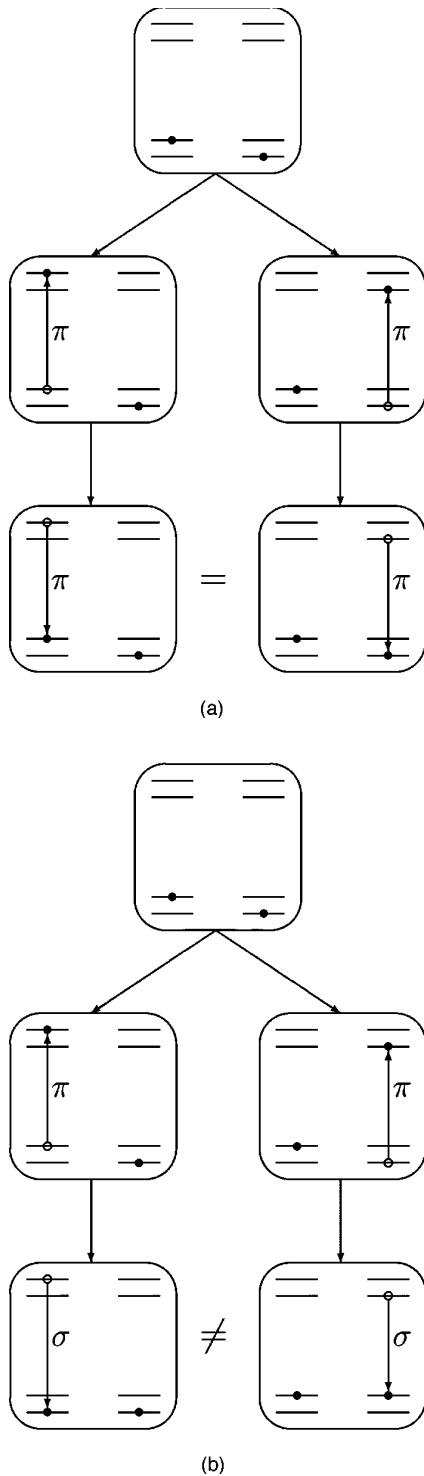
(a)

(b)

FIG. 4. Each box represents the combined state of the two ions. The ordering of energy levels is the same as in Fig. 2. In (a) (the π case), one ion or the other undergoes a π transition from the ground to the excited state. That ion undergoes a π transition back to the ground state. The two paths lead to the same final state of the two ions. Hence the probability amplitudes must be added and interference is possible. In (b) (the σ case), one ion or the other undergoes a π transition to the excited state, but the excited ion undergoes a σ transition to the ground state. The two paths lead to different final states of the two ions. Hence there is no possibility of interference. In order for interference to occur, it is *not* necessary that the initial states of the two ions be the same, only that the final combined states for the two paths be the same.
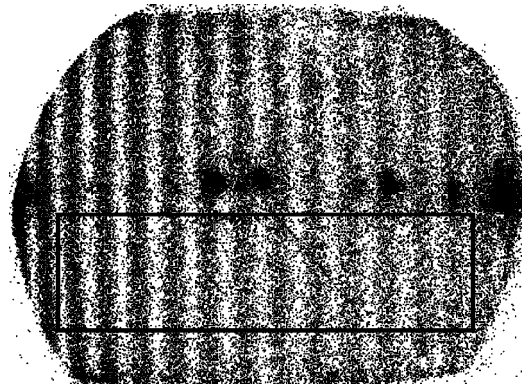

FIG. 5. Experimental fringe data for the case in which the detected light is polarized in the same direction as the incoming light (π case). The ion separation $d = 4.17$ μm. The angle ϕ (the deviation from the forward-scattering direction) increases to the right. The decrease in visibility with increasing ϕ is due to thermal motion of the ions. The dark spots are due to stray reflections of the laser beams. The data within the rectangle were summed along the vertical direction and least-squares fitted.

The spectrum of the light having polarization $\hat{\boldsymbol{\epsilon}}_\sigma$ does not contain a δ function. In the limit of low applied intensity, it is a Lorentzian having a width approximately equal to the photon scattering rate, which can be much less than the natural linewidth. Even for applied intensities approaching $s = 1$, the coherence length is on the order of c/γ, where γ is the spontaneous decay rate of the excited state. For the Hg$^+$ $6p$ $^2P_{1/2}$ level, this is about 70 cm. For interference fringes to exist, the radiation from the two atoms must be *mutually* coherent. Whether or not fringes should exist in the $\hat{\boldsymbol{\epsilon}}_\sigma$-polarized light from two atoms is not immediately obvious from a classical analysis. However, the perturbative quantum treatment of Sec. V predicts that there should be no interference since there is only one probability amplitude connecting the initial and final states. The absence of interference in this case is fundamentally a quantum effect, though one having more to do with the quantum nature of the atom and the existence of degenerate, orthogonal ground
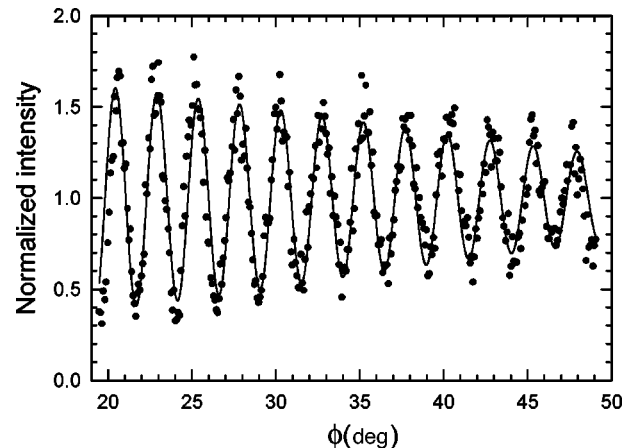

FIG. 6. Experimental fringe data (dots) from the image of Fig. 5 and a least-squares fit (line) to the sum of the theoretical intensity [Eq. (29)] and a constant background. The fitted temperature is approximately equal to the Doppler-cooling limit.

states, than with the quantum nature of the electromagnetic field. Precisely the same point was made by Scully and Drühl when they showed that interference fringes are not present in the Raman radiation emitted by two three-level atoms having a Λ configuration [3].

Wong et al. [13] calculated the interference of resonance fluorescence from two four-level atoms having a level structure like that of ^{198}Hg$^+$. Their analytic calculations are for a simpler geometry than the one actually used by Eichmann et al. [1] and ignore the motion of the ions. They do, however, include the effect of the decrease in visibility due to the incoherent component of the resonance fluorescence, which is not included in the perturbative calculation of Sec. V. The analytic calculations of Wong et al. and the present calculations agree in the limits in which they are both valid, that is, for low applied intensities and for no ion motion. In particular, Wong et al. show that the fringe visibility can approach 100% at low applied intensities, with polarization-selective detection. Wong et al. also made Monte Carlo wave-function simulations, in which the motion of the ions was included classically, and observed a decrease in visibility due to this effect.

Huang et al. [12] calculated the effect of thermal motion on the interference fringe visibility for two two-level atoms, each trapped in a separate harmonic well. They obtained an expression equivalent to Eq. (1) of Eichmann et al. [1] for this model. However, the treatment of Eichmann et al., the details of which are given in the present article, is more useful for the analysis of the experiment of Ref. [1] since it deals explicitly with the actual normal mode structure of the two trapped ions.

Brewer has published a theory of interference in the light scattered from two four-level atoms [11]. One prediction of this theory is that the fringe visibility cannot exceed 50%, even with polarization-selective detection. This contradicts the experimental results of Sec. VI shown in Fig. 6. While the maximum visibility is about 60%, only slightly exceeding 50%, no background has been subtracted from the data and there are several known sources of decreased visibility, including thermal motion of the ions, the incoherent component of the resonance fluorescence, and stray scattered light. The data were normalized by division by a slowly varying detection sensitivity function, a process that cannot enhance the visibility.

The basic flaw in Brewer's argument can be seen in Eq. (2) of Ref. [11], where he lists the basis states for the two-atom system. The states $|5\rangle$–$|8\rangle$ are the four states in which both atoms are in the ground electronic state. The states $|1\rangle$–$|4\rangle$ are linear combinations of states in which one atom is in the ground state and one is in the excited state. However, most of the possible states of this type are missing, apparently because of a false assumption that the allowed states must have a particular kind of exchange symmetry. For example, the intermediate superposition state shown in Fig. 4(a) is, in his notation,

$$\frac{1}{\sqrt{2}}(|c_1 b_2\rangle \pi_{nn,1} + |a_1 d_2\rangle \pi_{nn,2}) \qquad (44)$$

and is not contained in the list. The neglect of these basis states leads to the neglect of processes like that of Fig. 4(a),

in which the two atoms are initially in different m_J states. Thus he reaches the false conclusion that the two atoms must initially be in the same m_J state in order for interference to occur. Since he misses half of the processes that lead to interference, he predicts a maximum visibility, with polarization-sensitive detection, of 50% rather than 100%.

We conclude with some remarks regarding the principle of complementarity. Wave and particle properties of light are complementary and hence cannot be observed at the same time. If it is possible to determine which atom scattered the photon, the interference fringes must vanish. Feynman's thought experiments, in which various methods of determining the path of an electron through a two-slit Young interferometer lead to the destruction of interference fringes due to a random momentum transfer, are often quoted (see Ref. [2], pp. 1-6–1-11). However, in Chap. 3 of the same textbook, Feynman emphasizes the seemingly more fundamental viewpoint that interference is present only if there exist different indistinguishable ways to go from a given initial state to the same final state. His example of the scattering of neutrons from a crystal is very similar to the experiment of Eichmann et al. If the nuclei of the atoms in the crystal have a nonzero spin, the angular distribution of scattered neutrons is the sum of a featureless background and some sharp diffraction peaks. The sharp diffraction peaks are associated with neutrons that do not change their spin orientations in the scattering. The featureless background is associated with neutrons whose spins change their orientations in the scattering. In this case, there must also be a change in the spin orientation of one of the nuclei in the crystal. It would be possible in principle to determine the nucleus which scattered the neutron, so there is no interference.

APPENDIX: CALIBRATION OF THE SATURATION PARAMETER

For the case where an electric-dipole transition between a $^2S_{1/2}$ ground state and a $^2P_{1/2}$ excited state is excited by linearly polarized light, we define the saturation parameter s similarly to the way in which it is defined for a two-level system [26]. The magnetic field is assumed to be small and the quantization axis for the ion is along the electric field. We define

$$s = \frac{\Omega_1^2/2}{(\omega_0 - \omega_{\text{in}})^2 + (\gamma/2)^2}, \qquad (A1)$$

where $\Omega_1 = 6^{-1/2}|\mathcal{E}_0(^2S_{1/2}\|D^{(1)}\|^2P_{1/2})|\hbar^{-1}$ is the Rabi frequency, and the other terms have been defined previously. In order for the perturbative analysis of Sec. V to be valid, we

must have $s \ll 1$. In the case of Hg^+, the $^2P_{1/2}$ state has a small (approximately 10^{-7}) probability of decaying to the metastable $^2D_{3/2}$ state, which decays either directly to the ground state or to the metastable $^2D_{5/2}$ state, which decays to the ground state. The 194.2-nm fluorescence intensity from a single ion is bistable since it has a steady level when the ion is cycling between the $^2S_{1/2}$ and $^2P_{1/2}$ states and vanishes when the ion drops to a metastable state. The fractional population of the $^2P_{1/2}$ state, summed over both m_J values, is $s/2(1+s)$ while the ion is cycling between the $^2S_{1/2}$ and $^2P_{1/2}$ states. The quantum jump statistics have been discussed in several previous articles [15,27,28]. For a single ion, we define p_{on} to be the fraction of the time that the ion is cycling between the $^2S_{1/2}$ and $^2P_{1/2}$ states and $p_{off} = (1 - p_{on})$ to be the fraction of the time that it spends in either of the metastable states. It can be shown, from the steady-state solutions of the differential equations for the populations [Eqs. (2a)–(2c) of Ref. [28]], that s is related to the ratio p_{off}/p_{on} according to

$$\frac{1}{2}\frac{s}{(1+s)} = \frac{\gamma_1\gamma_2(p_{off}/p_{on})}{\gamma_3(\gamma_2+f_2\gamma_1)} \approx 0.36\,\frac{p_{off}}{p_{on}}, \qquad (A2)$$

where the parameters γ_1, γ_2, γ_3, and f_2 have been measured [15] and the uncertainty in the coefficient (0.36) is about 30%, due mostly to the uncertainty in γ_3.

For two ions, the fluorescence will be tristable since zero, one, or two ions may be in a metastable state. During an interference fringe measurement, the number of photons detected in each successive period of a few milliseconds was recorded. Figure 7 shows a plot of the probability distribution of the 5-ms photon counts during the measurement of Fig. 5. The three peaks correspond, from left to right, to two, one, or zero ions being in a metastable state. The leftmost peak corresponds to the signal from stray background light since there is no fluorescence from the ions. The curve is a least-squares fit to a sum of three Gaussians. The areas under
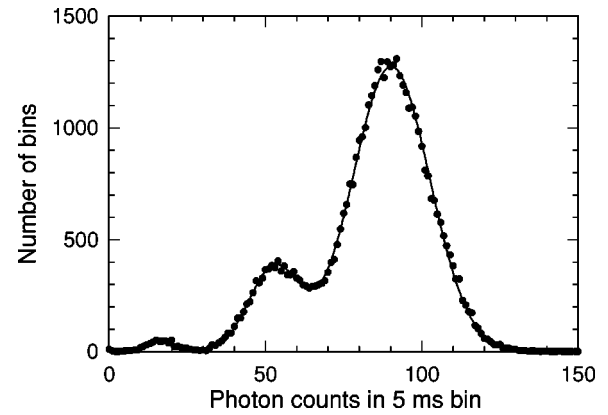

FIG. 7. Plot of the probability distribution of the fluorescence intensity for two ions, used to determine the saturation parameter s. The horizontal axis corresponds to the number of photons counted in a 5-ms interval. The vertical axis corresponds to the number of 5-ms intervals in which a given number of photons was counted. This was measured simultaneously with the interference fringes shown in Fig. 5. The curve is a least-squares fit to a sum of three Gaussians. The areas under the Gaussians, from left to right, are proportional to the probabilities that two, one, or none of the ions are in a metastable state. Higher values of s correspond to higher populations in the metastable states.

the peaks should be in the ratio $p_{off}^2 : 2p_{off}p_{on} : p_{on}^2$. The ratios of the areas obtained from the fit are 0.011:0.160:0.828, so $p_{off}/p_{on} = 0.10 \pm 0.01$ and, from Eq. (A2), $s = 0.078 \pm 0.025$, so the perturbative analysis should be a good approximation.

During this measurement period, the interference fringe detection was gated off for 5 ms if the number of photons detected in the previous 5 ms was less than 80. This helped to prevent loss of the fringe visibility due to background from single-ion fluorescence, which would have no interference fringes.

[1] U. Eichmann, J. C. Bergquist, J. J. Bollinger, J. M. Gilligan, W. M. Itano, D. J. Wineland, and M. G. Raizen, Phys. Rev. Lett. **70**, 2359 (1993).

[2] R. Feynman, R. Leighton, and M. Sands, *The Feynman Lectures on Physics* (Addison-Wesley, Reading, MA, 1965), Vol. III.

[3] M. O. Scully and K. Drühl, Phys. Rev. A **25**, 2208 (1982).

[4] P. Storey, S. Tan, M. Collet, and D. Walls, Nature (London) **367**, 626 (1994).

[5] E. P. Storey, S. M. Tan, M. J. Collet, and D. F. Walls, Nature (London) **375**, 368 (1995).

[6] H. W. Wiseman, F. E. Harrison, M. J. Collett, S. M. Tan, D. F. Walls, and R. B. Killip, Phys. Rev. A **56**, 55 (1997).

[7] M. O. Scully, B.-G. Englert, and H. Walther, Nature (London) **351**, 111 (1991).

[8] B.-G. Englert, M. O. Scully, and H. Walther, Nature (London) **375**, 367 (1995); Sci. Am. (Int. Ed.) **271**(6), 56 (1994).

[9] R. G. Brewer, Phys. Rev. A **52**, 2965 (1995).

[10] R. G. Brewer, Phys. Rev. A **53**, 2903 (1996).

[11] R. G. Brewer, Phys. Rev. Lett. **77**, 5153 (1996).

[12] H. Huang, G. S. Agarwal, and M. O. Scully, Opt. Commun. **127**, 243 (1996).

[13] T. Wong, S. M. Tan, M. J. Collett, and D. F. Walls, Phys. Rev. A **55**, 1288 (1997).

[14] M. G. Raizen, J. M. Gilligan, J. C. Bergquist, W. M. Itano, and D. J. Wineland, Phys. Rev. A **45**, 6493 (1992).

[15] W. M. Itano, J. C. Bergquist, R. G. Hulet, and D. J. Wineland, Phys. Rev. Lett. **59**, 2732 (1987).

[16] H. J. Lipkin, Ann. Phys. (N.Y.) **18**, 182 (1962).

[17] N. D. Mermin, J. Math. Phys. **7**, 1038 (1966).

[18] D. S. Bateman, S. K. Bose, B. Dutta-Roy, and M. Bhattacharyya, Am. J. Phys. **60**, 829 (1992).

[19] W. M. Itano and D. J. Wineland, Phys. Rev. A **25**, 35 (1982).

[20] D. Polder and M. F. H. Schuurmans, Phys. Rev. A **14**, 1468 (1976).

[21] W. Heitler, *The Quantum Theory of Radiation*, 3rd ed. (Oxford University Press, London, 1954), pp. 201 and 202.

[22] B. R. Mollow, Phys. Rev. **188**, 1969 (1969).

[23] J. T. Höffges, H. W. Baldauf, T. Eichler, S. R. Helmfrid, and H. Walther, Opt. Commun. **133**, 170 (1997).

[24] Th. Richter, Opt. Commun. **80**, 285 (1991).

[25] P. Kochan, H. J. Carmichael, P. R. Morrow, and M. G. Raizen, Phys. Rev. Lett. **75**, 45 (1995).

[26] C. Cohen-Tannoudji, J. Dupont-Roc, and G. Grynberg, *Atom-Photon Interactions* (Wiley, New York, 1992), p. 369.

[27] W. M. Itano, J. C. Bergquist, R. G. Hulet, and D. J. Wineland, Phys. Scr. **T22**, 79 (1988).

[28] W. M. Itano, J. C. Bergquist, and D. J. Wineland, Phys. Rev. A **38**, 559 (1988).